# Tat peptide–calmodulin binding studies and bioinformatics of HIV-1 protein–calmodulin interactions

**ARTICLE** *in* PROTEINS STRUCTURE FUNCTION AND BIOINFORMATICS · JULY 2011

Impact Factor: 2.63 · DOI: 10.1002/prot.23048



**8 AUTHORS**, INCLUDING:

Dung Hoang Nguyen
University of Manitoba
**6** PUBLICATIONS **63** CITATIONS
SEE PROFILE

Shaheen Shojania
University of British Columbia - Vancouver
**10** PUBLICATIONS **205** CITATIONS
SEE PROFILE

Kenneth G Standing
University of Manitoba
**151** PUBLICATIONS **6,108** CITATIONS
SEE PROFILE

PROTEINS
STRUCTURE ■ FUNCTION ■ BIOINFORMATICS

# Tat peptide-calmodulin binding studies and bioinformatics of HIV-1 protein–calmodulin interactions

Peter McQueen,[1] Lynda J. Donald,[1] Thach N. Vo,[1] Dung H. Nguyen,[1] Heather Griffiths,[1] Shaheen Shojania,[1] Kenneth G. Standing,[2] and Joe D. O'Neil[1]*

[1] Department of Chemistry, University of Manitoba, Winnipeg, Manitoba, Canada R3T 2N2
[2] Department of Physics & Astronomy, University of Manitoba, Winnipeg, Manitoba, Canada R3T 2N2

ABSTRACT

**The human immunodeficiency virus type 1 (HIV-1) genome encodes 18 proteins and 2 peptides. Four of these proteins encode high-affinity calmodulin-binding sites for which direct interactions with calmodulin have already been described. In this study, the HIV-1 proteome is queried using an algorithm that predicts calmodulin-binding sites revealing seven new putative calmodulin-binding sites including residues 34–56 of the transactivator of transcription (Tat). Tat is a 101-residue intrinsically disordered RNA-binding protein that plays a central role in the regulation of HIV-1 replication. Interactions between a Tat peptide (residues 34–56), melittin, a well-characterized calmodulin-binding peptide, and calmodulin were examined by direct binding studies, mass spectrometry, and fluorescence. The Tat peptide binds to both calcium-saturated and apo-calmodulin with a low micromolar affinity. Conformational changes induced in the Tat peptide were determined by circular dichroism, and residues in calmodulin that interact with the peptide were identified by HSQC NMR spectroscopy. Multiple interactions between HIV-1 proteins and calmodulin, a highly promiscuous signal transduction hub protein, may be an important mechanism by which the virus controls cell physiology.**

Proteins 2011; 79:2233–2246.


**Key words: bioinformatics; calmodulin; cell-cycle; circular dichroism; fluorescence; human immunodeficiency virus; mass spectrometry; melittin; NMR spectroscopy; transactivator of transcription.**

## INTRODUCTION

Calmodulin is an ubiquitous receptor for the second messenger $Ca^{2+}$ ion that regulates many metabolic pathways.[1] In humans, hundreds of proteins are known to bind calmodulin in calcium-dependent and calcium-independent mechanisms, yet the metabolic implications of these interactions are unknown for a majority of proteins.[2] Calmodulin recognizes a variety of sequence motifs in target proteins and binds in a variety of conformations regulated by the binding of 0, 2, or 4 calcium ions.[3] Many calmodulin-binding sequences in the targets are basic, amphipathic helices about 20 residues in length and are described using a nomenclature that refers to the distances separating two key bulky residues that are either 14, (1–16 motif), 12 (1–14 motif), or 8 (1–10 motif) residues apart, and may identify key hydrophobic residues (1-5-8-14 motif). The IQ motif is named after the first sequence (IQXXXRGXXXR) observed in myosin.[4] In addition, several proteins that bind calmodulin have sequences that do not fall into any of these categories.[3]

A recent survey of interactions between human proteins and the proteins of human pathogens indicates that viruses and bacteria mainly manipulate cell cycle, apoptosis, immune response, and nuclear transport.[5] Four HIV-1 proteins are known to interact with calmodulin. HIV-1 gp160 reportedly binds calmodulin in a process that is required for enhanced Fas-mediated apoptosis.[6,7] Near the C-terminus of the transmembrane protein gp41 are two calmodulin-binding sites[8] proposed to be involved in induction of apoptosis (see[9] and references therein) that could be an important mechanism by which CD4+-lymphocytes decline. Calmodulin binding by Env has also been proposed to play a key role in T-cell signaling important in viral replication,[8] and calmodulin levels are known to increase in cells expressing the envelope glycoprotein.[6,10] The matrix protein p17 (Gag) is a structural protein found on the interior surface of the viral membrane that participates in a number of activities from preintegration of the viral DNA into the host nucleus to assembly of new viral particles.[11] Matrix protein contains two contiguous high-affinity calmodulin-binding sites that bind calmodulin in a calcium-dependent

Additional Supporting Information may be found in the online version of this article.
Grant sponsors: Natural Sciences and Engineering Research Council of Canada, University of Manitoba
*Correspondence to: Joe O'Neil, Department of Chemistry, University of Manitoba, Winnipeg, Manitoba, Canada R3T 2N2. E-mail: joneil@cc.umanitoba.ca.
Received 29 October 2010; Revised 18 March 2011; Accepted 22 March 2011
Published online 1 April 2011 in Wiley Online Library (wileyonlinelibrary.com). DOI: 10.1002/prot.23048

manner.[10,12] Transient increases in cytoplasmic $Ca^{2+}$ have been shown to increase the amounts of HIV-1 Gag and the accumulation and release of virus-like particles in multivesicular bodies[13] suggesting that calmodulin binding to the matrix protein may regulate this process. HIV-1 Nef interacts with a large number of cell proteins, regulates protein trafficking, degradation, immune recognition, and signal transduction and is involved in CD4/MHC down regulation and T-cell activation but blocks apoptosis.[14] Nef binds calcium-saturated but not apocalmodulin with high affinity in a reaction that is enhanced 20-fold by Nef myristoylation.[15] Finally, the HIV-1 protease (PR, retropepsin) cleaves calcium-free calmodulin at two sites.[16,17]

The human immunodeficiency virus type 1 (HIV-1) transactivator of transcription (Tat) is essential for productive viral replication.[18,19] Tat stimulates elongation of full-length RNA transcripts by recruiting the cellular Positive Transcription Elongation Factor b (P-TEFb) that phosphorylates the C-terminal domain of RNA Polymerase II (RNAPII), components of Negative-TEF, and the transcription elongation factor Spt5.[20–23] Tat is a 101-residue RNA-binding protein encoded by two exons.[20,24] The first exon defines amino acids 1–72 and it activates transcription although with a lower proficiency than the full-length protein.[20,25–28] Solution NMR spectroscopy,[29] X-ray diffraction[30–32] and small angle X-ray scattering experiments[33] have confirmed that the protein exists in a mostly extended disordered conformation both free in solution and when bound to protein and RNA partners. Each of Tat's five sequence domains has been associated with multiple binding partners and biological activities[34–37] suggesting that the protein segments are exposed *in vivo*. In particular, the arginine-rich basic segment (residues 48–59) is responsible for binding the HIV-1 transactivation response (TAR) RNA,[38] contains a nuclear localization signal, and is a highly potent protein transduction domain.[39–42]

HIV-1 Tat has been implicated in host cell cycle, apoptosis, and immune response.[43,44] For example, Tat lengthens the G1 phase of the cell cycle and 10 human proteins involved in G1 are known to interact with Tat.[5] In addition, the Gln-rich region of Tat has been implicated in mitochondrial apoptosis of T-cells.[37] It is also well known that cells regulate many of the pathways involved in these processes using the second messenger calcium ion. Tat is a suspected contributor to the development of NeuroAIDS[45] and both HIV-1 Tat and Env have been proposed to cause neuronal cell death via disruption of calcium homeostasis although the mechanism by which this occurs is unknown.[46] By interacting with calmodulin, Tat and other vial proteins could control multiple metabolic pathways. Here, the HIV-1 proteome is queried using bioinformatics to identify potential calmodulin-binding sites in Tat and other HIV-1 proteins. Then, interactions between Tat and calmodulin are examined by peptide binding studies and spectroscopically. This interaction may provide a molecular explanation for Tat's multiple biological effects including its neurotoxicity.

## MATERIALS

Three peptides with the following sequences were used: Peptide-1: Acetyl-QVCFITKALGISYGRKKRRQR-$NH_2$ (Sigma, Fairlawn, NJ; $\epsilon_{280} = 1280\ M^{-1}\ cm^{-1}$), Peptide-2: Acetyl-FITKALGISYGRKKRRQR-$NH_2$ (CPC Scientific, San Jose, CA; $\epsilon_{280} = 1280\ M^{-1}\ cm^{-1}$), and Peptide-3: Acetyl-WGGGFITKALGISYGRKKRRQR-$NH_2$ (BioBasic, Markham, ON; $\epsilon_{280} = 6970\ M^{-1}\ cm^{-1}$) were 86%, 95%, and 95% pure according to electrospray ionization mass spectrometry and high-performance liquid chromatography. Peptide-3 was designed with an N-terminal tryptophan so that binding to calmodulin-sepharose could be monitored by absorption spectroscopy. Melittin, with the sequence GIGAVLKVLTTGLPALISWIKRKRQQ, was purchased from Sigma (Fairlawn, NJ; $\epsilon_{280} = 5690\ M^{-1}\ cm^{-1}$) and was 97% pure. Calmodulin was purchased from A.G. Scientific and was greater than 98% pure by SDS-PAGE. Uniformly $^{15}N$-labeled sea urchin calmodulin, which has the same sequence as vertebrate calmodulin, was expressed from a pET23d plasmid (Novagen, Madison, WI and a generous gift of Rachel Klevit, University of Washington and Andy Hudmon, Indiana University School of Medicine) in *E. coli* BL21(DE3)plysS cells[47] grown in M9 minimal medium supplemented with $^{15}NH_4Cl$ (Cambridge Isotope Laboratories, Andover, MA). It was purified by phenyl-sepharose chromatography.[48] Bovine serum albumin, sodium dodecylsulphate, Coomassie Brilliant Blue R-250, β-mercaptoethanol, Calmodulin-Agarose, EDTA, HEPES buffer, dansylchloride, ammonium acetate, and urea were obtained from Sigma-Aldrich (Fairlawn, NJ). Bis-Tris, glycerol, sodium sulphate, and Tris were from Fisher Scientific (Fairlawn, NJ). Bromophenol blue was from BDH (Toronto, ON). Ammonium acetate (99.999%) and dithiothreitol were from Aldrich Chemical (Milwaukee, WI). SDS-PAGE molecular weight markers were from Fermentas Life Sciences (Burlington, ON). All other materials were of the highest purity commercially available.

## METHODS

### Affinity chromatography

Calmodulin-Sepharose was equilibrated with 20 m*M* HEPES buffer at pH 7.0 containing 100 m*M* $Na_2SO_4$ and 2 m*M* $CaCl_2$. The manufacturer reports that the Calmodulin-Sepharose resin has a ligand density of 0.9–1.3 mg calmodulin per mL of drained resin but its binding capacity is reported as "unknown." Tat Peptide-3 and melittin dissolved in equilibration buffer were applied to 4.0 and 3.5 mL of settled equilibrated resin, respectively.

In a second experiment, the peptides were applied to equilibrated resins with volumes of 2.5 and 2.1 mL, respectively. The beads were then washed in turn with equilibration buffer, the equilibration buffer containing 4 m*M* or 40 m*M* EDTA but no calcium, and the same buffer containing 2% SDS but no calcium or EDTA. Eluted peptides were detected by tryptophan absorption at 280 nm using the extinction coefficients listed above in Methods.

### Preparation of dansyl-calmodulin

Dansyl-calmodulin was prepared as described.[49] Briefly, a 1-mL sample of 1 mg/mL calmodulin was brought to a concentration of 250 μ*M* $CaCl_2$ and then transferred to an amber bottle. 1 mg of dansylchloride was dissolved in 1 mL of acetone and then 2.5 μL of this solution was added to the calmodulin solution. The mixture was then stirred at room temperature for 90 min and then dialyzed twice against Tris buffer (50 m*M* Tris-HCl, pH 8.0, 0.2*M* NaCl, 0.2 m*M* EDTA). The absorbance at 340 nm was measured to determine the amount of dansyl group incorporated into calmodulin (molar extinction coefficient of dansyl chloride = 34,000 L $mol^{-1}$ $cm^{-1}$).

### Circular dichroism

CD spectra were obtained with a Jasco J810 CD spectropolarimeter. Calmodulin was prepared in 20 m*M* HEPES buffer at pH 7.0 containing 100 m*M* $Na_2SO_4$ at a concentration of about 50 μ*M* (1 mg/mL) and measured in a quartz cell with a 0.1-cm path length. Calmodulin concentrations were determined using the calculated molar absorptivity of 2560 $M^{-1}$ $cm^{-1}$. Stock solutions of Peptide-1 were prepared by weighing the peptides, dissolving them in the appropriate buffer and measuring their absorption at 280 nm. The peptide CD spectra were measured in a cell with a 0.5-cm path length. Sample temperature was controlled by a Julabo F25 circulating water bath. Protein spectra were collected at 20 nm/min between 240 and 180 nm with a response time of 4 s and a data pitch of 0.1 nm. Peptide spectra were collected at 5 nm/min with a 4-s response time. The CD intensity and wavelength of the spectropolarimeter were calibrated using solutions of D-10-camphorsulphonic acid.[50] Mean residue ellipticities ($[\theta] \times 10^{-3}$ deg cm–$^2$ $dmole^{-1}$) were calculated using the equation: $[\theta]_M = M\theta/(10)(l)(c)(n)$, where $M$ is relative mass in grams per mole, θ is the measured ellipticity in millidegrees, $l$ is the cell path length in dm, $c$ is the protein concentration in g/L, and $n$ is the number of residues.

### Fluorescence

The Jasco J810 spectropolarimeter is also equipped with a fluorescence detector. The fluorescence emission spectrum of dansyl-calmodulin was measured from 350 to 650 nm using a 1-cm path length quartz fluorescence cell. Calmodulin concentration was 0.51 μ*M* with approximately 80% of calmodulin molecules having bound dansylchloride (dansyl concentration = 0.41 μ*M*) based on the spectrophotometrically-measured concentrations of calmodulin and the dansyl group. Maximum emission was observed at about 496 nm.

### Mass spectrometry

Stock solutions at 50 μ*M* in nanopure water were prepared for calmodulin (CaM), melittin, and Tat Peptide-1. The stock buffer was 0.5*M* ammonium acetate (Aldrich 99.999%). Denatured calmodulin samples were 10–12 μ*M* in 2% acetic acid, 50% methanol and were sprayed from a 26-gauge metal capillary. For nanospray, samples were diluted to 1–2 μ*M* of each protein or peptide in 50 m*M* ammonium acetate, and 3–5 μL of sample was loaded into a New Objective PicoTip™ cut to the appropriate length. This capillary was then installed in a custom-built holder, and spray voltage was adjusted to 1 kV above the declustering voltage. For every sample, only the declustering voltage was varied to assess the stability of the complex. A constant backpressure of 2 psi was applied to the capillary to keep the sample flowing and a fresh capillary was used for every sample.[51] All the noncovalent complexes were analyzed on an orthogonal electrospray time-of-flight instrument built in the Department of Physics and Astronomy at the University of Manitoba.[52] Details will be given in the appropriate figure caption. For MALDI analysis, peptide stock solution at 1 mg/mL was mixed with an equal volume of DHB matrix on a metal target. MALDI spectra were acquired on a QqTOF instrument that has been described.[53]

### NMR spectroscopy

$^{15}$N-labeled calmodulin, prepared as described earlier, was dissolved in 10 m*M* HEPES buffer, 6 m*M* $CaCl_2$, 0.1*M* KCl, 5% v/v $D_2O$ at pH 7.0. The CaM concentration was 0.5 m*M*, and Tat Peptide-2 was added in 0.2 molar equivalents from a stock solution dissolved in water. HSQC NMR spectra were acquired with a 600 MHz Varian INOVA spectrometer equipped with a triple resonance probe head at 20.2°C and the standard Varian BioPack pulse sequence.[54] The NMR probe was calibrated with methanol,[55] and all spectra were processed with NMRPipe.[56] Spectra were apodized using a squared cosine bell function, zero filled to twice the data set size, and linear predicted (forward-backward with eight prediction coefficients) prior to Fourier transformation. The dimensions of the resulting processed data sets were 1024 × 512. The pulse sequences used are sensitivity-enhanced and use gradients for coherence selection and water suppression.[57] $^{15}$N decoupling during acquisition was done using the WALTZ-16 sequence[58] with a 7.196 kHz field

**Table I**
Predicted Calmodulin-Binding Sites in HIV-1 Proteins and Protein Transduction Peptides

| Protein (precursor) | Sequence | Motif | Net Q |
|---|---|---|---|
| Matrix p17 (Gag) | [21]LRPGGKKKYKLKHIVWASRELERFAVNPGLL | Unclassified[60] | 6.1 |
| Capsid p24 (Gag) | [122]PPIPVGEIYKRWIILGLNKIVRMYSPTSI | Unclassified[60] | 2.9 |
| Retropepsin p10 (Pol) | [41]RWKPKMIGGIGGFIKVRQYDQILI | Unclassified[60] | 3.9 |
| RT RNase H domain p66 (Pol) | [441]YVDGAANRETKLGKAGYVTNRGRQKVVTLTD | Unclassified[60] | 2.9 |
| Integrase p31 (Pol) | [171]HLKTAVQMAVFIHNFKRKGGIGGYSA | Unclassified[60] | 4.4 |
| Vif | [139]HNKVGSLQYLALAALITPKKI | Unclassified[60] | 3.1 |
| Tat | [34]CQVCFITKALGISYGRKKRRQRR | Unclassified[60] | 7.8 |
| Vpu | [19]AIVVWSIVIIEYRKILRQRKIDRLI | Unclassified[60] | 3.9 |
| gp160 (Env) | [10]LWRWGWRWGTMLLGMLMIC'S | 1-5-8-14[60] | 1.9 |
| gp120 (Env) | [158]SFNISTSIRGKVQKEYAFFYKLDIIPI | Unclassified[60] | 1.9 |
| gp41 (Env) | [257]YHRLRDLLLIVTRIVELLGRRGW | Unclassified[60] | 3.2 |
| Nef | [87]LSHFLKEKGGLEGLIHSQRR | Unclassified[60] | 2.4 |
| Transportan/Mastoparan | [14]INLKALAALAKKIL | 1-14 motif[42] | 2.9 |
| P1 | [5]LHLLVLAAALQGAWSQPKK | Unclassified[42] | 2.1 |
| HSV-1 VP22 | [267]DAATATRGRSAASRPTERRAPARSASRPRRPVE | None[42] | 5.9 |
| Penetratin from Antennapedia | [43]RQIKIWFQNRRMKWKK | None[42] | 6.9 |
| Melittin | [1]GIGAVLKVLTTGLPALISWIKRKRQQ | 1-8-14 | 4.9 |

Table I lists the calmodulin-binding site sequences and motifs identified by the Calmodulin Target Database tool[61] in HIV-1 proteins[60] and four protein transduction domains[42] and the net charges (Q) on the peptides. Precursor polyproteins are identified in brackets following the name(s) of the proteins. The reference HXB2 HIV-1 strain amino acid numbering are used.[60] The signal peptide cleavage site in gp160 is indicated by C'S.

strength. $^{1}$H chemical shifts were referenced to the water signal that resonates 4.821 ppm from 2,2-dimethyl-2-silapentane-5-sulfonate (DSS) at 293 K.[55] $^{15}$N referencing was done indirectly relative to DSS as recommended.[59]

## RESULTS

### HIV-1 proteome analysis

The HIV-1 proteome is small enough (3 precursor polyproteins, 15 proteins, and 2 peptides) that the individual protein sequences obtained from the Los Alamos HIV database[60] (http://www.hiv.lanl.gov/) could be manually submitted to the Calmodulin Target Database[61] (http://calcium.uhnres.utoronto.ca/ctdb) and the results individually analyzed. The binding site analysis tool first searches a database of known calmodulin-binding sequences and provides a classification of the binding motif when positive results are returned. The tool then searches protein sequences for new calmodulin-binding sites using a set of criteria that includes sequence hydropathy, α-helical propensity, residue weight, residue charge, hydrophobic residue content, helical class, and occurrence of particular residues. Table I shows that 12 HIV-1 proteins are predicted to contain calmodulin-binding sites. When queried, the database already contained four HIV-1 calmodulin-binding sequences from gp160, gp120, gp41, and Nef. The viral envelope glycoproteins are synthesized as a precursor polypeptide (gp160). Processing of gp160 releases a leader sequence and two proteins, gp120 and gp41, that form a noncovalent complex on the surface of the virus. The N-terminal calmodulin-binding segment in gp160 is classified as a 1-5-8-14 motif. Interestingly, the N-terminal gp160 motif is proteolytically removed during maturation of the protein at C's (Table I). Nothing is known about the possible function of the high-affinity CaM-binding peptide before or after its release from the protein. The other 3 sites in gp120, gp41, and Nef are unclassified.

The binding site analysis tool also predicted a CaM binding site in the matrix protein from residues 21 to 51. In this case binding studies have localized two contiguous CaM binding sites in matrix to residues 11–25 and 31–46 that show substantial overlap with the prediction.[62] It is important to point out that the actual CaM-binding site residues in matrix based on a structure of the complex have not been determined.[12] The tool also predicted seven new putative high-affinity calmodulin-binding sites in the HIV-1 proteome in Capsid, Retropepsin, Reverse Transcriptase RNase H domain, Integrase, Vif, Tat, and Vpu (Table I). Of these, Capsid has been tested for calmodulin binding and was found not to bind.[62] Only HIV-1 proteins p6, nucleocapsid, p51 Reverse Transcriptase, Vpr, and Rev do not appear to contain any high-affinity calmodulin-binding sites and neither do the two peptide products p1 (16 residues) and p2 (14 residues). Remarkably about 10% of the amino acids in the HIV-1 proteome encode putative high-affinity calmodulin-binding sites.

As discussed earlier, we examined four protein transduction domains (PTD) to determine if the binding site tool is able to distinguish between PTD's and CaM binding sites. The 14 residue stretch of the peptide Transportan[42] is present in the Calmodulin Target Database and identified as having a 1–14 motif. Furthermore, the synthetic peptide P1[42] contains a 19-residue stretch that is identified as a putative CaM-binding region. However, the well-characterized protein transduction domains from Herpes Simplex Virus, VP22, and the C-helix from

the *Antennapedia* homeodomain (Penetratin) are not predicted to bind calmodulin. Thus, while some features of protein transduction domains are similar to calmodulin-binding sites apparently the binding-site analysis tool is able to differentiate between CaM binding sites and protein transduction domains.

### Calmodulin-agarose binding assays

Wherever possible in this work calmodulin-binding studies were done with bee venom melittin, a well-characterized high-affinity, $Ca^{2+}$-dependent calmodulin-binding peptide, for comparison to the Tat peptides. Preliminary experiments to determine if Tat peptide binds to calmodulin were conducted by Calmodulin-Agarose affinity chromatography. To increase the detection sensitivity by ultraviolet absorption, Tat Peptide-3 contains an N-terminal tryptophan residue linked by three glycines to a peptide with the same sequence as Peptide-1. In one experiment, 49 nmoles of Peptide-3 were added to 2.5 mL of calmodulin–sepharose resin; 33 nmoles of peptide eluted in 40 m*M* EDTA and 23 nmoles eluted when the resin was washed with buffer containing SDS. Similar results were obtained with melittin. These experiments illustrate that the peptide from Tat binds calcium-saturated calmodulin and that some of it is released when calmodulin undergoes a conformational change upon the release of calcium. It is not clear from these experiments if the peptides released by washing with SDS-containing buffer are bound to apo-calmodulin or nonspecifically adsorbed to the resin or column material.

### Mass spectrometry

Electrospray ionization of denatured CaM was done to verify the identity of the protein. The mass spectrum of denatured CaM and its deconvolution yield a mass of 16,706 ± 4 Da indicating that the N-terminal Met has been removed (theoretical mass 16706.348). Melittin (monoisotopic mass 2844.5 Da) and the Tat Peptide-1 (monoisotopic mass 2548.5 Da) were verified by MALDI mass spectrometry (data not shown).

Nanospray mass spectrometry was used to measure the formation of calmodulin-peptide complexes. Supporting Information Figure S1 shows a nanospray mass spectrum of 1 μ*M* calmodulin in 5 μ*M* calcium acetate at a declustering voltage of 250 V. The labeled peaks represent calmodulin with five (*m/z* 3372), six (*m/z* 2810), and seven (*m/z* 2408) positive charges. Even at a relatively high declustering voltage of 250 V the calmodulin remains folded, although there is some evidence of denatured protein in the lower *m/z* region. Deconvolution of the three labeled ions is shown in the inset spectrum where the heavy arrow indicates the expected mass for apo-calmodulin. The most abundant peak is at 16,859 ± 4 Da and closely corresponds to a protein with four bound calcium ions (theoretical average mass 16,866.66 Da). The other masses shown fit reasonably well with expected values for calmodulin plus two (16,783 Da), three (16,822 Da), and five (16,900 Da) bound calcium ions. Unlabeled ions are probably additional adducts of sodium. Full details of the observed and expected ions can be found in Supporting Information Table SI.

Figure 1(A–C) shows the effects of increasing the declustering voltage on the distribution of ions present in a mixture of 1 μ*M* calmodulin, 1 μ*M* melittin, and 10 μ*M* calcium. At low voltage (Panel A), two overlapping ion envelopes are present that correspond to two species with masses of 16,873 Da (free CaM) and 19,704 Da (CaM + melittin), respectively. There is one distinct 8+ ion from the complex (marked with an arrow) but the 7+ complex ion and the 6+ ion of free CaM that have nearly identical *m/z* values and appear here as a single peak. As the declustering voltage is increased, (Panels B and C), the 8+ ion from the complex (arrow) decreases in intensity relative to the free CaM 7+ ion, and two new ions appear at *m/z* 1423 (2+ of free melittin) and 4219 (4+ of CaM). At the highest applied voltage (Panel C), the $8^+$ ion from the complex is almost gone (arrow) with the main part of the spectrum having one ion envelope from calmodulin and an increase in abundance of the 2+ ion at *m/z* 1423.405 with a calculated monoisotopic mass of 2844.8 Da. A 3+ ion at *m/z* 949.282 (calculated mass 2844.8 Da) is not shown due to the high background in the spectrum from salts. These data can be interpreted as follows: ions at *m/z* 2463.823 and 2815.645 (8+ and 7+ positive charges respectively) arise from the formation of a complex of one melittin, one calmodulin, and four calcium ions (theoretical mass 19,714.13). At higher voltages the ions from the complex are less abundant and only the calcium-saturated calmodulin 6+ and 7+ ions are present at *m/z* 2815.645 and 2409.188, respectively. At low voltage, no free melittin ions are observed, but, as the voltage is increased, the 2+ and 3+ melittin ions appear, and the charge envelope of the free calmodulin changes because of charge splitting between the two components of the complex. For instance, the new 4+ ion of calmodulin and the new 3+ ion of melittin likely arose from the 7+ ion of the complex observed at 80 V. Not detectable in the spectra are any free melittin ions that were not bound to calcium-saturated CaM during electrospraying because their multiple charges would place them in the spectra below $m/z$ = 1000 where they would be obscured by the background.

Similar results were obtained with a mixture of 1 μ*M* calmodulin, 1.5 μ*M* Tat Peptide-1, and 5 μ*M* calcium. At low declustering voltage (Fig. 1 Panel D), there appear to be only two major ions, at *m/z* 2400 and 2700. Expansion of those regions gives clear evidence for two major ion envelopes—the 6+ and 7+ of calculated mass 16873 Da, and the 7+ and 8+ (at *m/z* 2773.457 and 2427.340, respectively) of calculated mass 19409 Da. When the

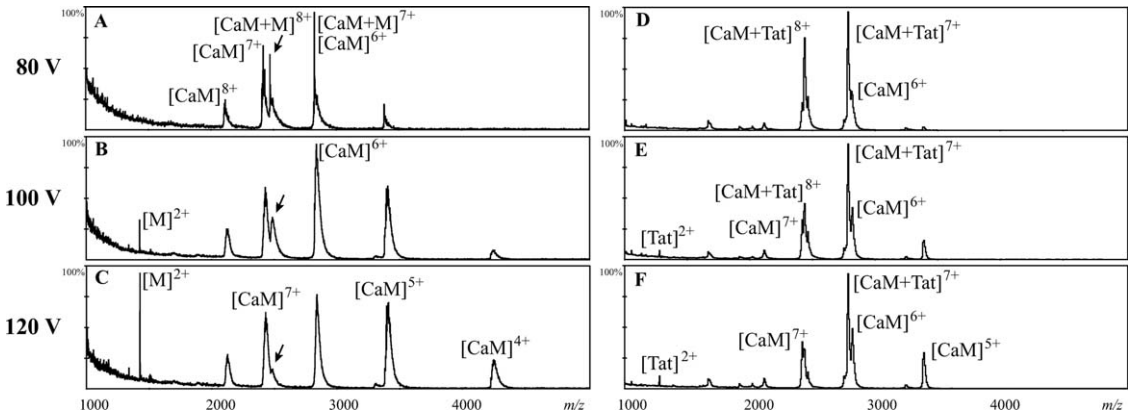


**Figure 1**

A representative series of nanospray spectra at increasing declustering voltage of a sample made with 1 μ*M* calmodulin (CaM), 1 μ*M* melittin (M), and 10 μ*M* calcium acetate in 50 m*M* ammonium acetate (Panels **A**–**C**) and 1 μ*M* CaM, 1.5 μ*M* Tat Peptide-1, 5 μ*M* calcium acetate in 50 m*M* ammonium acetate (Panels **D**–**F**). Panel A: At 80 V there are four ion clusters in the spectrum, with two overlapping charge envelopes. The ion series labeled CaM has an average mass of 16,873 Da and the ion series labeled CaM + M has an average mass of 19,704 Da. (Deconvolution is not possible because of the overlapping ion envelopes). Panel B: At 100 V, the $[CaM + M]^{8+}$ ion at *m/z* 2500 is less abundant (marked by an arrow), and there is a new 2+ melittin ion at *m/z* 1423.403 (calculated mass 2844.8 Da). Panel C: At 120 V, the major ions are only those from calmodulin and melittin. Also indicated are the 4+ and 5+ ions of the calmodulin. Panel D: At 80 V, there appear to be only two ions present in the spectrum—*m/z* 2400 and 2800. Manual calculation gives an average mass of 19,409 Da for the complex ion, and 16,873 Da for free CaM. Panel E: At 100 V, the ions from the larger species are less abundant relative to those of the ions from the smaller species, and there is a new 2+ ion at *m/z* 1275.286. Panel F: At 120 V, the spectrum has changed only slightly, significant Tat-CaM complex is still present and free Tat peptide is increased only slightly at *m/z* 1275.286.

declustering voltage is increased to 100 V (Panel E) both ion envelopes are still present, and there is a new doubly-charged ion at *m/z* 1275.286 (calculated mass 2548.6 Da). Further increase of the voltage (Panel F) changes the spectrum only slightly in marked contrast to the complete loss of the complex that was observed at 120 V for calmodulin and melittin [Fig. 1(C)]. At the lower range of the spectrum, a new 2+ ion is now apparent, with a calculated mass of 2548.6 Da. The absence of free Tat peptide ions in Panel D suggests that the free peptide ions observed in Panels E and F arise from collisionally-induced decomposition of the complex in the mass spectrometer. Unbound peptide would likely have been multiply charged and unobservable because of the high background at $m/z < 800$.

## Circular dichroism and fluorescence

Figure 2 shows the CD spectrum of calcium-saturated calmodulin (dashed line) showing the characteristics of a predominantly α-helical protein with negative bands at 222 nm and 208 nm, a positive band at 190 nm, and a cross-over point at 201 nm.[63] Addition of one mole equivalent of Tat Peptide-1 (Fig. 2, solid line) causes a small increase in negative and positive ellipticity frequently observed when calmodulin-binding peptides bind calmodulin and indicative of a small increase in the helicity of the mixture. The CD spectrum of Tat peptide alone (Fig. 2 inset) has a strong negative band at 198 nm and weak positive ellipticity between 212 and 222 nm indicating that the peptide adopts a disordered conformation in the absence of CaM. Since the overall helical content of calmodulin is usually unchanged in the presence and absence of bound peptide, the results suggest that the Tat peptide has adopted a helical conformation upon binding to calmodulin.[64,65] This is confirmed by subtraction of the CD spectrum of free CaM from the spectrum of CaM in the presence of the Tat peptide which yields a spectrum with negative peaks at 208 and

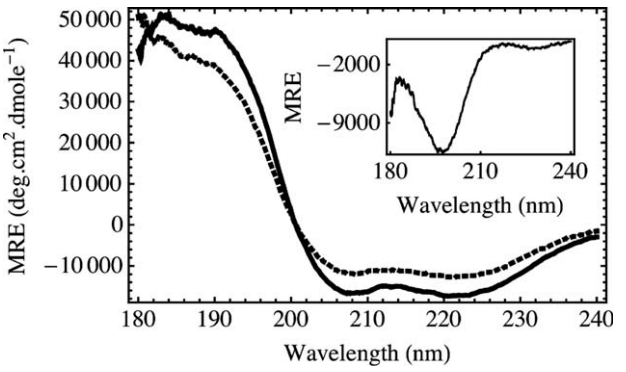


**Figure 2**

Far ultraviolet CD spectra of 50 μ*M* $Ca^{2+}$-calmodulin in the absence (dashed line) and presence (solid line) of Tat Peptide-1 showing the characteristic negative α-helical peaks at 208 nm and 222 nm, respectively. The inset spectrum shows the CD spectrum of Tat peptide alone exhibiting a negative peak at 200 nm characteristic of disordered protein.

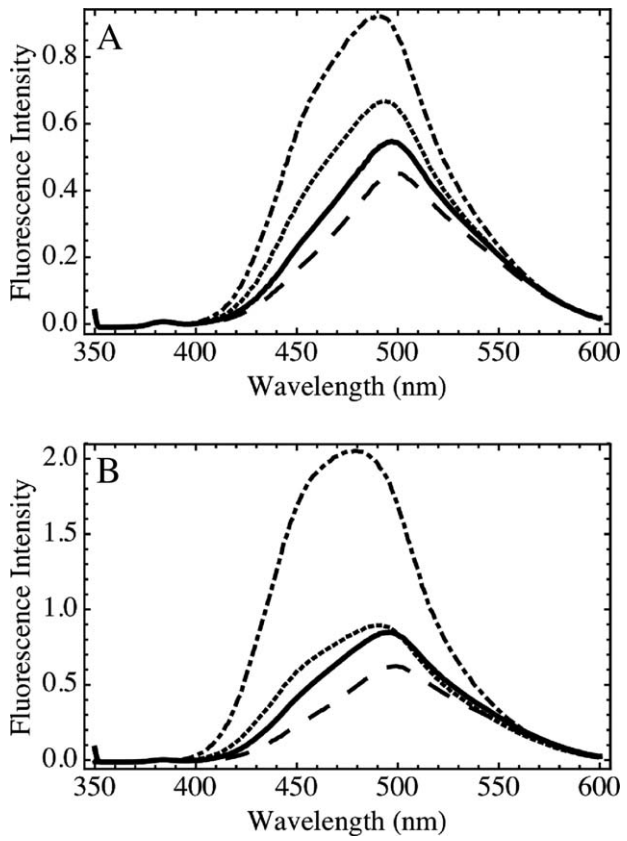


**Figure 3**

Fluorescence emission from apo-dansyl-calmodulin (solid lines), upon the addition of EDTA (dashed lines), upon addition of Tat Peptide-1 (Panel A, dotted line) or melittin (Panel B, dotted line) and upon addition of calcium (dot-dashed lines).

220 nm and a positive peak at 190 nm (data not shown) indicating the increased helical content of the mixture upon Tat peptide binding to CaM. Nearly identical behavior was observed when melittin was added to calmodulin although the ellipticity change was slightly greater upon the binding of melittin (data not shown).

Figure 3 Panel A (solid line) show the fluorescence spectrum of dansyl-calmodulin with an emission maximum at 500 nm. Addition of EDTA (dashed line) quenches the fluorescence slightly indicative of a conformational change in CaM owing to the removal of residual calcium. Addition of Tat Peptide-1 results in an enhancement and blue shift of the dansyl-CaM fluorescence (dotted line) indicating affinity of the Tat peptide for apo-calmodulin. However, the affinity of the Tat peptide for calmodulin is enhanced by addition of calcium in excess of the added EDTA as evidenced by the significantly enhanced dansyl fluorescence with a maximum at 490 nm (dash-dot line). Very similar results were obtained when melittin was added to dansyl-calmodulin. The spectra in Figure 3 Panel B show that like the Tat peptide, melittin binds to apo-calmodulin (dotted line) and to calcium-saturated calmodulin (dash-dot line) however the fluorescence enhancement when melittin binds dansyl-CaM is significantly greater when melittin binds than when Tat peptide binds.

### HSQC NMR spectroscopy

The conformational changes induced in calmodulin by Tat peptide binding were measured by $^{1}H/^{15}N$ HSQC NMR spectroscopy. Addition of Tat Peptide-2 in 0.2 mol equivalent portions relative to calcium-saturated CaM resulted in slight line broadening of most of the CaM resonances and upon the addition of 1 mol equivalent of peptide some precipitate was observed. This is in contrast to the previously described spectroscopic binding experiments that were done at protein and peptide concentrations 10- to 500-fold lower than those used for the NMR experiments. Figure 4 Panel A shows HSQC spectra of $^{15}N$-calmodulin in the absence (red) and presence (blue) of 0.4 mol equivalents of Tat Peptide-2. The fact that only one set of peaks is observed when peptide is added to CaM means that peptide is in rapid exchange between calmodulin-bound and calmodulin-free states. For this experiment, the relevant NMR timescale is determined by the chemical shift differences between the bound and free calmodulin resonances ($2\pi\Delta\nu$) and indicates that the peptide on- and off-binding rates must be around 600 $s^{-1}$ or faster.

The resonance peaks in Figure 4 were assigned by comparison to the published assignments of $Ca^{2+}$-calmodulin[66]; the observed resonances in the absence of Tat peptide are in excellent agreement with the published values. Because calmodulin is predominantly helical, protein chemical shift dispersion is low and there is significant spectral overlap between the spectra of the bound and free CaM. As a consequence, only the well-resolved and unambiguously assigned peaks were used to determine the calmodulin residues perturbed by the binding of Tat peptide. Examination of the well-dispersed peaks shows that the largest chemical shift changes occur at residues K13, L18, K21, T26, I27, T29, G33, L39, and A57 whereas I100, T117, I130, G134, V136, and N137 are relatively unaffected by the binding of peptide. Figure 4 Panel B shows the structure (PDB ID: 1LIN) of calcium-saturated CaM bound to trifluoperazine.[67] The red residues indicate backbone amide resonances that undergo chemical shift changes in the presence of Tat Peptide-2. The chemical shifts of the blue residues are relatively unaffected by Tat peptide binding. From these results, it appears that the Tat peptide preferentially binds to the N-terminal calcium-binding domain of calmodulin.

## DISCUSSION

### HIV-1 proteins and calmodulin

Not only HIV-1 but also many other viruses have very simple genomes that encode only a small number of

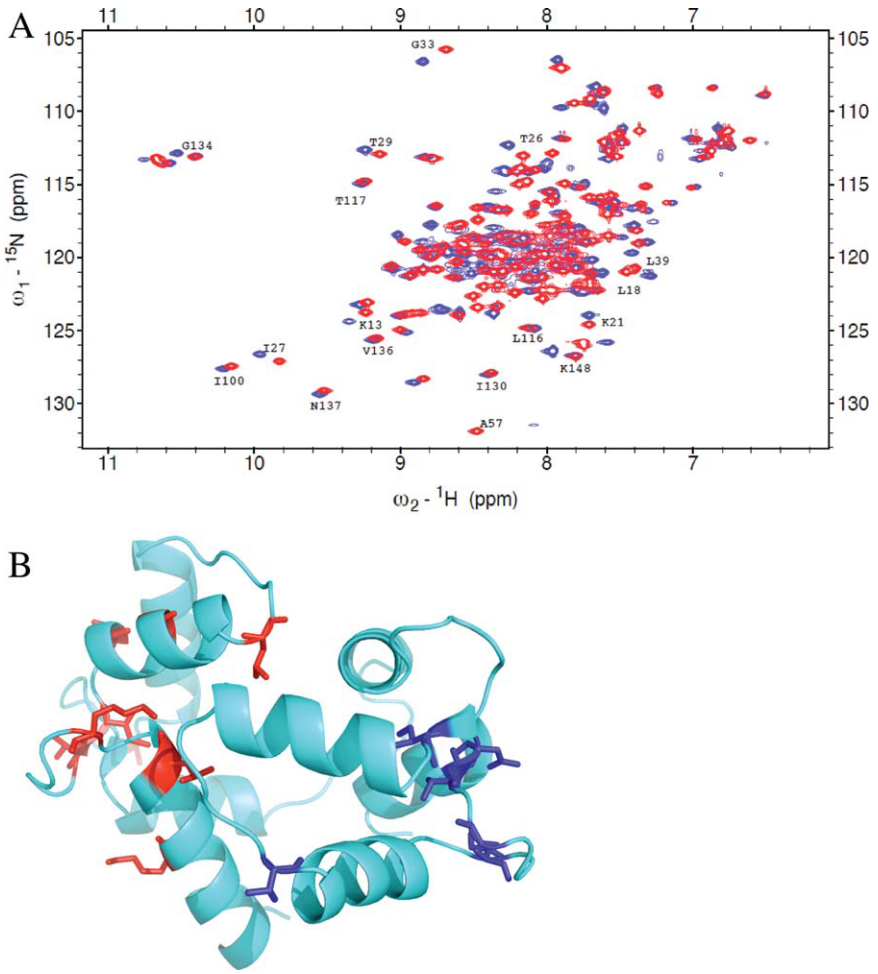


**Figure 4**

Panel **A** shows HSQC spectra of $^{15}$N-calmodulin in the absence (red) and presence (blue) of Tat Peptide-2. Assignments are based on reference.[69] Panel **B** shows the structure (PDBID: 1LIN) of calcium-saturated CaM bound to trifluoperazine.[67] The red residues (N-terminus; K13, L18, K21, T26, I27, T29, G33, L39, and A57) indicate backbone amide resonances that undergo large chemical shift changes in the presence of Tat peptide. The chemical shifts of the blue residues (C-terminus; I100, T117, I130, G134, V136, and N137) are relatively unaffected by Tat peptide binding.

proteins and therefore have limited biological machinery. Viruses must therefore commandeer the infected host-cell machinery in order to replicate. One solution to this problem is multifunctional viral proteins capable of interacting with multiple host proteins. A recent survey of interactions between human proteins and the proteins of human pathogens, including HIV-1, indicates that viruses and bacteria mainly manipulate host cell cycle, apoptosis, immune response, and nuclear transport.[68] The HIV-1 Human Protein Interaction Database[69–71] at the National Center for Biological Interaction (NCBI) lists 1443 interactions between host proteins and the 18 proteins of HIV-1. This type of binding promiscuity has sometimes been referred to as "moonlighting,"[72] and it appears to be an important strategy by which viruses control host cell physiology and replicate new virions.

The human immunodeficiency virus type 1 (HIV-1) genome is highly compact encoding only 18 proteins and two peptides,[14] and on the order of 3000 amino acids. Remarkably, four of these proteins, Matrix,[10,12] Nef,[15] and the membrane glycoproteins gp160[6,7] and gp41[8,14] encode high-affinity calmodulin-binding sites for which direct interactions with calmodulin have already been reported. Perhaps more remarkable is that application of an algorithm to predict calmodulin binding sites in the HIV-1 proteome revealed seven additional putative calmodulin-binding proteins. Altogether, more than 10% of the amino acids encoded by the genome are putative calmodulin-binding sites and it will be of interest to examine each of these proteins for possible interactions with CaM both *in vitro* and *in vivo* to determine which are legitimate CaM-binding proteins and what physiological relevance CaM-binding has to the pathology of cellular HIV-1 infection. Mutagenesis studies suggest that calmodulin is optimized for low specificity enabling it to

bind to a large number of targets with a range of affinities.[73] This would suggest that many of the identified binding sites in Table I are likely to be legitimate CaM-binding sites. It is possible of course that protein folding could bury some or all of a putative CaM-binding site to prevent its interaction with CaM but the net positive charges on all the sites (Table I) suggests that they are exposed in the folded proteins.

Protein–protein interaction networks are scale-free with most proteins having one or a small number interactions and a few proteins, hubs, making tens and hundreds of interactions with other proteins.[74,75] Calmodulin is a well-known hub protein that interacts with hundreds of other cellular and foreign proteins.[1–3,74] Conformational flexibility appears to be the key to calmodulin's binding promiscuity. Intrinsic disorder in the linker that connects the N- and C-terminal calcium-binding domains in CaM permits the protein to adopt many distinct conformations that adapt it to a large variety of target proteins.[76] It is not surprising then that HIV-1 would target calmodulin, an important hub protein, to control key aspects of cellular physiology. Space does not permit speculation on all the possible physiological roles of CaM binding by all of the HIV-1 proteins identified in Table I. However, one aspect of CaM regulation is worth mentioning. It is now recognized that protein signaling pathways do not consist of a fixed set of interconnected proteins and enzymes but rather that connectivity can be ephemeral resulting from transient protein localization and concentration fluctuations that can sometimes lead to diametrically opposed phenotypes.[77] In line with this concept it has been suggested that calmodulin is a limiting factor in cell signaling[78] and that competition between CaM-binding proteins, in addition to transient calcium fluctuations, can lower free CaM concentrations to less than 200 nM and thereby determine the cell state.[79] In fact just such a mechanism of action has been proposed for regulator of calmodulin signaling (RCS). Phosphorylation by protein kinase A (PKA) increases its affinity for $Ca^{2+}$-calmodulin so that it acts as a competitive inhibitor for numerous $Ca^{2+}$-calmodulin-dependent proteins and enzymes.[79] Neuromodulin and neurogranin are further examples of calmodulin-binding proteins that regulate the availability of calmodulin. They release calmodulin in response to phosphorylation by protein kinase C or A.[80] It is even possible that HIV-1 proteolyses calmodulin in cells in an effort to lower CaM concentration as, *in vitro*, the HIV-1 protease cleaves calcium-free calmodulin at two sites.[16,17] In summary, the present proteome analysis suggests that HIV-1 controls cell physiology by multiple interactions with CaM, a highly promiscuous signal transduction hub protein.

## Tat and calmodulin

Recent bioinformatics analyses suggest that up to 30% of the eukaryotic proteome is intrinsically disordered under physiological conditions[81,82]; that is, in the absence of binding partners these proteins, or protein segments, do not fold into a stable conformation but rather exist in a more or less restricted ensemble of conformations determined by the amino acid sequence. These analyses also indicate that viruses have the highest fraction of proteins containing a disordered segment (37%) compared to bacteria (30%), eukaryotes (21%), and archaea (19%).[81] Intrinsically disordered proteins are particularly well suited to serving as hub proteins because their larger surface areas can permit multiple and even simultaneous interactions with interaction partners.[83–85]

The present bioinformatics analysis suggests that HIV-1 Tat contains one CaM-binding site. Nanospray mass spectrometry confirmed that a peptide corresponding to the identified CaM-binding site binds to $(Ca^{2+})_4$-calmodulin similar to the well-known calmodulin-binding peptide melittin. The detection by mass spectrometry and fluorescence of Tat peptide-calmodulin complexes at low micromolar concentrations suggests that the $K_d$ for the complex is on the order of $10^{-6}$ $M$ or lower. The $[CaM+Melittin]^{7+}$ complex is significantly dissociated at 100 V [Fig. 1(B)], whereas the $[CaM+Tat]^{7+}$ complex is mostly intact at a declustering voltage of 120 V [Fig. 1(F)] suggesting that the Tat peptide may bind slightly more tightly to CaM than does melittin whose dissociation constant is about $10^{-8}$ $M$.[86,87] Nevertheless, caution is advisable for several reasons[86] when interpreting soft-ionization mass spectrometric data for the determination of noncovalent binding affinities. Furthermore, if Tat peptide binds calmodulin with an affinity similar to that of melittin then the fast exchanging NMR resonances [Fig. 4(A)] require an association rate constant on the order of $6 \times 10^{10}$ $M^{-1}/s^{-1}$ making it more plausible that the binding affinity is on the low micromolar scale. On-rates near the diffusion limit may be explained by a significant contribution from the high net positive charge on the peptide and diffusion-limited on-rates were also observed for an isomer of a myosin light chain kinase peptide that also exhibited a high affinity but small chemical shift perturbations to CaM backbone amide resonances.[88] Finally, note that Tat peptides were studied because the full-length protein contains 7 Cys residues, and it is highly prone to oxidative multimerization and is much less soluble than are the peptides. Although it will be important to study the interaction between the full length Tat protein and CaM, Tat is an intrinsically disordered protein[29,33] and it is very unlikely that folding could bury the CaM-binding site.[30–32]

Both the Tat peptide and melittin perturbed dansyl-calmodulin fluorescence similarly indicating a binding interaction (see Fig. 3). The slightly larger enhancement of dansyl emission by melittin binding may indicate a difference in the interaction sites. One possibility is that melittin uses more hydrophobic contacts in its binding interface with CaM, whereas the Tat peptide may use

more electrostatic interactions. This speculation is in line with the more basic and less hydrophobic nature of the Tat peptide compared to melittin which has three fewer positive charges at pH 7 than the Tat peptide (Table I).

Circular dichroism spectropolarimetry showed that Tat peptide exits in an ensemble of unfolded conformations alone but adopts a helical conformation upon binding to CaM (see Fig. 2).[64,65] NMR spectroscopy studies of Tat-protein show that the region corresponding to the CaM-binding site in Tat is disordered.[29] However, binding-induced folding is a hallmark of many IDP's.[89] and the basic segment of Tat is induced to form a helix that binds to the major groove of the TAR stem-loop structure in the EIAV Tat-TAR-cyclin T1 complex.[31] This suggests that the basic segment is poised to form a helix upon interaction with binding partners and would fit with a conformational selection model of protein–protein interactions where a binding partner selects from among the ensemble of conformations of its ligand the most suitable binding conformation.[90,91] Because of its essential role in the life cycle of the virus, Tat is a highly attractive target for vaccine development.[92] However, peptides are usually far less immunogenic than the proteins from which they are derived.[93] Conformational restriction of peptides can lead to higher immunogenicity[94,95] and the present results suggests that residues 34–56 of Tat may be a suitable vaccine target because of the helical propensity of that region of the protein.

$^{15}$N-HSQC NMR spectroscopy identified residues mainly in the N-terminus of CaM involved in the binding of Tat peptide (see Fig. 4); however, it is clear that both domains of CaM are affected by Tat peptide binding as most of the resonances are observed to broaden. Interestingly, CaM resonance broadening was also observed for an IQ motif peptide from the intrinsically disordered protein PEP-19[96] and for melittin binding to apo-calmodulin.[87] As mentioned, calmodulin adopts a number of different conformations to enable it to bind to a variety of targets.[90] In many cases, peptide and protein binding causes a collapse of the extended conformation of calcium-saturated calmodulin to a globular conformation owing to dynamic flexibility of the helical linker in CaM.[90,97] Also, peptide:CaM binding stoichiometry is usually 1:1 but there are exceptions; for example, the first CaM-binding motif in Matrix binds with a 2:1 stoichiometry to the extended conformation of CaM.[98] The overall NMR resonance line broadening observed upon the addition of Tat peptide is likely not explainable by the increased effective mass of the complex but rather more likely reflects a change in the dynamics of the calmodulin conformational ensemble induced by the peptide binding. The chemical shift perturbation experiment shown in Figure 4(A) does not permit the assignment of a conformation for the Tat-CaM complex but it does suggest that the conformation of the N-terminus is more perturbed than that of the C-terminus. Clearly, further structural studies will be required to determine the conformation of CaM that binds HIV-1 Tat peptides and protein.

Because the predicted CaM-binding site in Tat contains the cell-penetrating protein transduction segment, we investigated whether the Calmodulin Target Database algorithm[61] can distinguish between PTD's and CaM-binding sites. The results in Table I suggest that two known PTD's are predicted not to be CaM-binding sites whereas two contain both functions. Interestingly, HIV-1 Rev contains a potent protein transduction domain[99] but is predicted not to contain a calmodulin-binding site. Thus, while some features of protein transduction domains are similar to calmodulin-binding sites apparently, the binding-site analysis tool is able to differentiate between CaM-binding sites and protein transduction domains. As far as we are aware, only in the case of Tat has a functional role been ascribed to a protein transduction domain. A major event in the progression of HIV-1 infection is neuronal damage despite the fact that neurons cannot be infected with the virus.[100] Tat can be released from infected microglia and astrocytes within the central nervous system (CNS)[101] and is able to cross the blood-brain barrier[102] resulting in cell death of neurons.[45,103] NeuroAIDS encompasses a range of disorders arising from damage to the peripheral and central nervous systems including HIV-associated dementia (HAD) and HIV-associated encephalitis (HIVE).[101,104] Several HIV-1 proteins have been implicated in neural dysfunction including gp120, gp41, Rev, Nef, and Tat.[103] However, it remains to be proven that enough Tat is released by infected cells to account for the observed pathology[105] and over-activation of the immune system, and in particular macrophages, may be the main contributor to neuropathy.[106] It therefore remains possible that the cell-penetrating properties of Tat are an artifact.

As discussed earlier for HIV-1 proteins in general, the ability of Tat to modulate $Ca^{2+}$-calmodulin-regulated signaling pathways will depend on the kinetics of the concentration and localization of Tat and CaM in a cell. However, a number of possible roles for Tat-CaM interactions in transcription activation, host cell cycle, apoptosis, and immune response can be proposed. For example, Tat activates transcription by recruiting cyclin-dependent kinases to the HIV-1 promoter.[20–23] $Ca^{2+}$-calmodulin activates calcineurin, a serine/threonine-specific protein phosphatase, which activates protein phosphatase 1 to dephosphorylate CDK9.[107] Tat modifies the activity of CDK9 to phosphorylate serine 5 of the RNA polymerase II carboxyl-terminal domain[108] so binding of $Ca^{2+}$-calmodulin by Tat could increase the amount of CDK9 for transcription activation. A further possibility is suggested by the role for $Ca^{2+}$-calmodulin-stimulated calcineurin and protein phosphatase1a in the release of P-TEFb from the 7SK snRNP that has been proposed recently.[109]

The role of intracellular calcium signaling in T-lymphocyte activation has been known for some time.[110] Tat has been proposed to contribute to immune suppression[44] by several different mechanisms; for example, Tat blocks calcium entry and phagocytosis by dendritic cells.[111] The Tat RGD domain blocks the activation of calcium-calmodulin kinase II (CAMKII) by β3-integrin in dendritic cells[111] preventing engulfment of apoptotic tumor cells. However, the basic domain of Tat showed no effect on CAMKII[111] activity. Furthermore, Tat inhibits L-type calcium channels and IL-12 secretion in dendritic cells,[112] but the effect appears to be mediated by residues 65–80 that do not include the CaM-binding segment. Since p38 MAP kinase phosphorylation of STAT1 is required for interferon-induced transcriptional activation (IFN-α and IFN-γ)[113] a plausible function for calmodulin-binding by HIV-1 Tat is regulation of the IFN-mediated immune response through calcium/calmodulin-dependent protein kinase II phosphorylation of STAT1.[114] The $Ca^{2+}$-CaM regulated phosphatase calcineurin plays a key role in regulating the transcription factor NF-AT during T-cell activation and it is conceivable that binding of Tat could interfere with this process.[1]

HIV-1 Tat lengthens the G1 phase of the cell cycle and ten human proteins involved in G1 are known to interact with Tat.[5] Tat may have a role in modulating cell cycle *via* $Ca^{2+}$-calmodulin regulation of calcineurin and CaMKII.[115] In general, disruption of calcineurin and CaMKII leads to cell cycle arrest. Through its binding to integrin receptors Tat has also been shown to induce the transition from G0 to G1 phase in quiescent T-cells increasing the efficiency of HIV-1 infection.[116] A human inhibitor of $Ca^{2+}$-calmodulin kinase II arrests the cell cycle and is deactivated by MEK/ERK.[117] The intrinsically disordered PEP-19 prevents cellular apoptosis from calcium overload by increasing the number of residues in CaM involved in millisecond to microsecond conformational exchange and altering calcium binding rates and cooperativity.[118] Tat may play a similar role as the Tat peptide increases calmodulin conformational exchange [Fig. 4(A)] and it has also been shown to prevent apoptosis.[119] Finally, the NIH HIV interactome reports a direct interaction between Tat and $Ca^{2+}$-calmodulin-dependent protein kinase I[69–71] that may be pertinent to Tat's role in NeuroAIDS.[120]

## ACKNOWLEDGMENTS

We thank Dr. Kirk Marat for assistance with the operation of the NMR spectrometer.

## REFERENCES

1. Hoeflich KP, Ikura M. Calmodulin in action: diversity in target recognition and activation mechanisms. Cell 2002;108:739–742.
2. Shen XC, Valencia CA, Szostak JW, Dong B, Liu RH. Scanning the human proteome for calmodulin-binding proteins. Proc Natl Acad Sci USA 2005;102:9734–9734.
3. Ishida H, Vogel HJ. Protein-peptide interaction studies demonstrate the versatility of calmodulin target protein binding. Protein Pept Lett 2006;13:455–465.
4. Bahler M, Rhoads A. Calmodulin signaling via the IQ motif. FEBS Lett 2002;513:107–113.
5. Dyer MD, Murali TM, Sobral BW. The landscape of human proteins interacting with viruses and other pathogens. PLOS Pathogens 2008;4:1–14.
6. Micoli KJ, Pan G, Wu Y, Williams JP, Cook WJ, McDonald JM. Requirement of calmodulin binding by HIV-1 gp160 for enhanced FAS-mediated apoptosis. J Biol Chem 2000;275:1233–1240.
7. Micoli KJ, Mamaeva O, Piller SC, Barker JL, Pan G, Hunter E, McDonald JM. Point mutations in the C-terminus of HIV-1 gp160 reduce apoptosis and calmodulin binding without affecting viral replication. Virology 2006;344:468–479.
8. Srinivas SK, Srinivas RV, Anantharamaiah GM, Compans RW, Segrest JP. Cytosolic domain of the human-immunodeficiency-virus envelope glycoproteins binds to calmodulin and inhibits calmodulin-regulated proteins. J Biol Chem 1993;268:22895–22899.
9. Shacklett BL, Weber CJ, Shaw KES, Keddie EM, Gardner MB, Sonigo P, Luciw PA. The intracytoplasmic domain of the Env transmembrane protein is a locus for attenuation of simian immunodeficiency virus SIVmac in rhesus macaques. J Virol 2000;74:5836–5844.
10. Radding W, Williams JP, McKenna MA, Tummala R, Hunter E, Tytler EM, McDonald JM. Calmodulin and HIV type 1: interactions with gag and gag products. AIDS Res Hum Retroviruses 2000;16:1519–1525.
11. De Francesco MA, Baronio M, Fiorentini S, Signorini C, Bonfanti C, Poiesi C, Popovic M, Grassi M, Garrafa E, Bozzo L, Lewis GK, Licenziati S, Gallo RC, Caruso A. HIV-1 matrix protein p17 increases the production of proinflammatory cytokines and counteracts IL-4 activity by binding to a cellular receptor. Proc Natl Acad Sci USA 2002;99:9972–9977.
12. Ghanam RH, Fernandez TF, Fledderman EL, Saad JS. Binding of calmodulin to the HIV-1 matrix protein triggers myristate exposure. J Biol Chem 2010;285:41911–41920.
13. Perlman M, Resh MD. Identification of an intracellular trafficking and assembly pathway for HIV-1 gag. Traffic 2006;7:731–745.
14. Swanson CM, Malim MH. SnapShot: HIV-1 proteins. Cell 2008;133:798.
15. Matsubara M, Tao J, Kawamura K, Shimojo N, Titani K, Hashimoto K, Hayashi N. Myristoyl moiety of HIV Nef is involved in regulation of the interaction with calmodulin in vivo. Protein Sci 2005;14:494–503.
16. Tomasselli aG, Howe WJ, Hui JO, Sawyer TK, Reardon IM, Decamp DL, Craik CS, Heinrikson RL. Calcium-free calmodulin is a substrate of proteases from human immunodeficiency virus-1 and virus-2. Proteins: Struct Funct Genet 1991;10:1–9.
17. Daube H, Billich a, Mann K, Schramm HJ. Cleavage of phosphorylase-kinase and calcium-free calmodulin by HIV-1 protease. Biochem Biophys Res Commun 1991;178:892–898.
18. Arya SK, Guo C, Josephs SF, Wong-Staal F. Trans-activator gene of human T-lymphotropic virus type III (HTLV-III). Science 1985;229:69–73.
19. Shojania S, O'Neil JD. Intrinsic disorder and function of the HIV-1 Tat protein. Protein Pept Lett 2010;17:999–1011.
20. Jeang KT, Xiao H, Rich EA. Multifaceted activities of the HIV-1 transactivator of transcription. Tat J Biol Chem 1999;274:28837–28840.
21. Yamaguchi Y, Takagi T, Wada T, Yano K, Furuya A, Sugimoto S, Hasegawa J, Handa H. NELF, a multisubunit complex containing RD, cooperates with DSIF to repress RNA polymerase II elongation. Cell 1999;97:41–51.
22. Bourgeois CF, Kim YK, Churcher MJ, West MJ, Karn J. Spt5 cooperates with human immunodeficiency virus type 1 Tat by preventing premature RNA release at terminator sequences. Mol Cell Biol 2002;22:1079–1093.

23. Kim YK, Bourgeois CF, Isel C, Churcher MJ, Karn J. Phosphorylation of the RNA polymerase II carboxyl-terminal domain by CDK9 is directly responsible for human immunodeficiency virus type 1 Tat-activated transcriptional elongation. Mol Cell Biol 2002; 22:4622–4637.
24. Neuveut C, Jeang KT. Recombinant human immunodeficiency virus type 1 genomes with tat unconstrained by overlapping reading frames reveal residues in Tat important for replication in tissue culture. J Virol 1996;70:5572–5581.
25. Kuppuswamy M, Subramanian T, Srinivasan A, Chinnadurai G. Multiple functional domains of Tat, the trans-activator of HIV-1. Mutat Anal Nucl Acids Res 1989;17:3551–3561.
26. Garcia Ja, Harrich D, Pearson L, Mitsuyasu R, Gaynor RB. Functional domains required for tat-induced transcriptional activation of the HIV-1 long terminal repeat. EMBO J 1988;7:3143–3147.
27. Smith SM, Pentlicky S, Klase Z, Singh M, Neuveut C, Lu CY, Reitz MS Jr, Yarchoan R, Marx PA, Jeang KT. An in vivo replication-important function in the second coding exon of Tat is constrained against mutation despite cytotoxic T lymphocyte selection. J Biol Chem 2003;278:44816–44825.
28. Mahlknecht U, Dichamp I, Varin A, Van Lint C, Herbein G. NF-kappaB-dependent control of HIV-1 transcription by the second coding exon of Tat in T cells. J Leukoc Biol 2008;83:718–727.
29. Shojania S, O'Neil JD. HIV-1 Tat is a natively unfolded protein—the solution conformation and dynamics of reduced HIV-1 Tat-(1–72) by NMR spectroscopy. J Biol Chem 2006;281:8347–8356.
30. Anand K, Schulte A, Fujinaga K, Scheffzek K, Geyer M. Cyclin box structure of the P-TEFb subunit cyclin T1 derived from a fusion complex with EIAV Tat. J Mol Biol 2007;370:826–836.
31. Anand K, Schulte A, Vogel-Bachmayr K, Scheffzek K, Geyer M. Structural insights into the Cyclin T1-Tat-TAR RNA transcription activation complex from EIAV. Nature Struct Mol Biol 2008;15:1287–1292.
32. Tahirov TH, Babayeva ND, Varzavand K, Cooper JJ, Sedore SC, Price DH. Crystal structure of HIV-1 Tat complexed with human P-TEFb. Nature 2010;465:747–751.
33. Foucault M, Mayol K, Receveur-Bréchot V, Bussat MC, Klinguer-Hamour C, Verrier B, Beck A, Haser R, Gouet P, Guillon C. UV and X-ray structural studies of a 101-residue long Tat protein from a HIV-1 primary isolate and of its mutated, detoxified, vaccine candidate. Proteins: Struct Funct Bioinform 2010;78:1441–1456.
34. Vendel AC, Lumb KJ. Molecular recognition of the human coactivator CBP by the HIV-1 transcriptional activator Tat. Biochemistry 2003;42:910–916.
35. Bieniasz PD, Grdina TA, Bogerd HP, Cullen BR. Recruitment of a protein complex containing Tat and cyclin T1 to TAR governs the species specificity of HIV-1 Tat. EMBO J 1998;17:7056–7065.
36. Chen D, Wang M, Zhou S, Zhou Q. HIV-1 Tat targets microtubules to induce apoptosis, a process promoted by the pro-apoptotic Bcl-2 relative Bim. EMBO J 2002;21:6801–6810.
37. Campbell GR, Pasquier E, Watkins J, Bourgarel-Rey V, Peyrot V, Esquieu D, Barbier P, de Mareuil J, Braguer D, Kaleebu P, Yirrell DL, Loret EP. The glutamine-rich region of the HIV-1 Tat protein is involved in T-cell apoptosis. J Biol Chem 2004;279:48197–48204.
38. Weeks KM, Ampe C, Schultz SC, Steitz TA, Crothers DM. Fragments of the HIV-1 Tat protein specifically bind TAR RNA. Science 1990;249:1281–1285.
39. Gupta B, Levchenko TS, Torchilin VP. Intracellular delivery of large molecules and small particles by cell-penetrating proteins and peptides. Adv Drug Deliv Rev 2005;57:637–651.
40. Cardarelli F, Serresi M, Bizzarri R, Beltram F. Tuning the transport properties of HIV-1 tat arginine-rich motif in living cells. Traffic 2008;9:528–539.
41. Derse D, Carvalho M, Carroll R, Peterlin BM. A minimal lentivirus Tat. J Virol 1991;65:7012–7015.
42. Deshayes S, Morris MC, Divita G, Heitz F. Cell-penetrating peptides: tools for intracellular delivery of therapeutics. Cell Mol Life Sci 2005;62:1839–1849.
43. Alimonti JB, Ball TB, Fowke KR. Mechanisms of CD4+ T lymphocyte cell death in human immunodeficiency virus infection and AIDS. J Gen Virol 2003;84 (Part 7):1649–1661.
44. Gallo RC. Tat as one key to HIV-induced immune pathogenesis and Tat (correction of Pat) toxoid as an important component of a vaccine. Proc Natl Acad Sci USA 1999;96:8324–8326.
45. Pocernich CB, Sultana R, Mohmmad-Abdul H, Nath A, Butterfield DA. HIV-dementia, Tat-induced oxidative stress, and antioxidant therapeutic considerations. Brain Res Brain Res Rev 2005:50.
46. Mattson MP, Haughey NJ, Nath A. Cell death in HIV dementia. Cell Death and Differentiation 2005;12:893–904.
47. Singla SI, Hudmon A, Goldberg JM, Smith JL, Schulman H. Molecular characterization of calmodulin trapping by calcium/calmodulin-dependent protein kinase II. J Biol Chem 2001;276: 29353–29360.
48. Gopalakrishna R, Anderson WB. Ca2+-induced hydrophobic site on calmodulin: application for purification of calmodulin by phenyl-Sepharose affinity chromatography. Biochem Biophys Res Commun 1982;104:830–836.
49. Kincaid RL, Billingsley ML, Vaughan M. Preparation of fluorescent, cross-linking, and biotinylated calmodulin derivatives and their use in studies of calmodulin-activated phosphodiesterase and protein phosphatase. Methods Enzymol 1988;159:605–626.
50. Wu CS, Chen GC. Adsorption of proteins onto glass surfaces and its effect on the intensity of circular dichroism spectra. Anal Biochem 1989;177:178–182.
51. Donald LJ, Duckworth HW, Standing KG. Mass Spectrometry in noncovalent protein interactions and protein assemblies. In: Celis J, Simons K, Small JV, Hunter T, Shotton D, editors.Cell biology—a laboratory handbook, 3rd ed., Vol.4. San Diego: Elsevier Academic Press; 2006. pp 457–464.
52. Kozlovski KI DL, Montero-Collado V, Loboda AV, Chernushevich IV, Ens W, Standing KG. TOF Mass spectrometer with ESI source, orthogonal injection, and 16 kV acceleration voltage, for study of noncovalent complexes. San Antonio, Texas: American Society for Mass Spectrometry; 2005. p 03:20.
53. Loboda AV, Krutchinsky AN, Bromirski M, Ens W, Standing KG. A tandem quadrupole/time-of-flight mass spectrometer with a matrix-assisted laser desorption/ionization source: design and performance. Rapid Commun Mass Spectrometry 2000;14:1047–1057.
54. Kay LE, Keifer P, Saarinen T. Pure absorption gradient enhanced heteronuclear single quantum correlation spectroscopy with improved sensitivity. J Am Chem Soc 1992;114:10663–10665.
55. Cavanagh JF, Wayne J, Palmer AG III, Skelton NJ. Protein NMR spectroscopy: principles and practise. San Diego: Academic Press; 1996.
56. Delaglio F, Grzesiek S, Vuister GW, Zhu G, Pfeifer J, Bax A. NMRPipe: a multidimensional spectral processing system based on UNIX pipes. J Biomol NMR 1995;6:277–293.
57. Farrow NA, Muhandiram R, Singer AU, Pascal SM, Kay CM, Gish G, Shoelson SE, Pawson T, Forman-Kay JD, Kay LE. Backbone dynamics of a free and phosphopeptide-complexed Src homology 2 domain studied by 15N NMR relaxation. Biochemistry 1994;33:5984–6003.
58. Shaka AJ, Keeler J, Frenkiel T, Freeman R. An improved sequence for broad-band decoupling—Waltz-16. J Magn Reson 1983;52:335–338.
59. Wishart DS, Bigam CG, Yao J, Abildgaard F, Dyson HJ, Oldfield E, Markley JL, Sykes BD. 1H, 13C and 15N chemical shift referencing in biomolecular NMR. J Biomol NMR 1995;6:135–140.
60. Leitner T, Foley B, Hahn B, Marx P, McCutchan F, Mellors J, Wolinsky S, Korber B, editors. HIV sequence compendium 2005. Theoretical Biology and Biophysics Group, Los Alamos National Laboratory, NM; 2005.
61. Yap KL, Kim J, Truong K, Sherman M, Yuan T, Ikura M. Calmodulin target database. J Struct Funct Genomics 2000;1:8–14.
62. Radding W, Williams JP, McKenna MA, Tummala R, Hunter E, Tytler EM, McDonald JM. Calmodulin and HIV type 1: interactions with Gag and Gag products. AIDS Res Hum Retroviruses 2000;16:1519–1525.

63. Fasman GD. Distinguishing transmembrane helices from peripheral helices by circular dichrosim. Biotechnol Appl Biochem 1993;18 (Part 2):111–138.
64. Zhou Y, Yang W, Lurtz MM, Ye Y, Huang Y, Lee HW, Chen Y, Louis CF, Yang JJ. Identification of the calmodulin binding domain of connexin 43. J Biol Chem 2007;282:35005–35017.
65. Salerno JC, Harris DE, Irizarry K, Patel B, Morales AJ, Smith SM, Martasek P, Roman LJ, Masters BS, Jones CL, Weissman BA, Lane P, Liu Q, Gross SS. An autoinhibitory control element defines calcium-regulated isoforms of nitric oxide synthase. J Biol Chem 1997;272:29769–29777.
66. Ikura M, Kay LE, Bax a. A novel-approach for sequential assignment of H-1, C-13, and N-15 spectra of larger proteins—heteronuclear triple-resonance 3-dimensional NMR-spectroscopy—application to calmodulin. Biochemistry 1990;29:4659–4667.
67. Vandonselaar M, Hickie RA, Quail JW, Delbaere LT. Trifluoperazine-induced conformational change in Ca(2+)-calmodulin. Nat Struct Biol 1994;1:795–801.
68. Dyer MD, Murali TM, Sobral BW. The landscape of human proteins interacting with viruses and other pathogens. PLoS Pathogens 2008;4:e32.
69. Fu W, Sanders-Beer BE, Katz KS, Maglott DR, Pruitt KD, Ptak RG. Human immunodeficiency virus type 1, human protein interaction database at NCBI. Nucleic Acids Res 2009;37(Database issue): D417–D422.
70. Ptak RG, Fu W, Sanders-Beer BE, Dickerson JE, Pinney JW, Robertson DL, Rozanov MN, Katz KS, Maglott DR, Pruitt KD, Dieffenbach CW. Cataloguing the HIV-1 human protein interaction network. AIDS Res Hum Retroviruses 2008;24:1497–1502.
71. Pinney JW, Dickerson JE, Fu W, Sanders-Beer BE, Ptak RG, Robertson DL. HIV-host interactions: a map of viral perturbation of the host system. AIDS 2009;23:549–554.
72. Jeffery CJ. Moonlighting proteins-an update. Mol Bio Syst 2009;5: 345–350.
73. Shifman JM, Mayo SL. Exploring the origins of binding specificity through the computational redesign of calmodulin. Proc Natl Acad Sci USA 2003;100:13274–13279.
74. Patil A, Kinoshita K, Nakamura H. Hub promiscuity in protein-protein interaction networks. Int J Mol Sci 2010;11:1930–1943.
75. Koonin EV, Wolf YI, Karev GP. The structure of the protein universe and genome evolution. Nature 2002;420:218–223.
76. Wilson MA, Brunger AT. The 1.0 A crystal structure of Ca(2+)-bound calmodulin: an analysis of disorder and implications for functionally relevant plasticity. J Mol Biol 2000;301:1237–1256.
77. Hahn KM, Kuhlman B. Hold me tightly LOV. Nat Methods 2010; 7:595–597.
78. Persechini A, Stemmer PM. Calmodulin is a limiting factor in the cell. Trends Cardiovasc Med 2002;12:32–37.
79. Rakhilin SV, Olson PA, Nishi A, Starkova NN, Fienberg AA, Nairn AC, Surmeier DJ, Greengard P. A network of control mediated by regulator of calcium/calmodulin-dependent signaling. Science 2004;306:698–701.
80. Xia ZG, Storm DR. The role of calmodulin as a signal integrator for synaptic plasticity. Nature Rev Neurosci 2005;6:267–276.
81. Chen JW, Romero P, Uversky VN, Dunker AK. Conservation of intrinsic disorder in protein domains and families. I. A database of conserved predicted disordered regions. J Proteome Res 2006;5: 879–887.
82. Ward JJ, Sodhi JS, McGuffin LJ, Buxton BF, Jones DT. Prediction and functional analysis of native disorder in proteins from the three kingdoms of life. J Mol Biol 2004;337:635–645.
83. Gunasekaran K, Tsai CJ, Kumar S, Zanuy D, Nussinov R. Extended disordered proteins: targeting function with less scaffold. Trends Biochem Sci 2003;28:81–85.
84. Dunker AK, Cortese MS, Romero P, Iakoucheva LM, Uversky VN. Flexible nets—the roles of intrinsic disorder in protein interaction networks. FEBS J 2005;272:5129–5148.
85. Patil A, Kinoshita K, Nakamura H. Domain distribution and intrinsic disorder in hubs in the human protein-protein interaction network. Protein Sci 2010;19:1461–1468.
86. Mathur S, Badertscher M, Scott M, Zenobi R. Critical evaluation of mass spectrometric measurement of dissociation constants: accuracy and cross-validation against surface plasmon resonance and circular dichroism for the calmodulin-melittin system. Phys Chem Chem Phys 2007;9:6187–6198.
87. Newman RA, Van Scyoc WS, Sorensen BR, Jaren OR, Shea MA. Interdomain cooperativity of calmodulin bound to melittin preferentially increases calcium affinity of sites I and II. Proteins 2008; 71:1792–1812.
88. Fisher PJ, Prendergast FG, Ehrhardt MR, Urbauer JL, Wand AJ, Sedarous SS, McCormick DJ, Buckley PJ. Calmodulin interacts with amphiphilic peptides composed of all D-amino acids. Nature 1994;368:651–653.
89. Tompa P. Intrinsically unstructured proteins. Trends Biochem Sci 2002;27:527–533.
90. Henzler-Wildman K, Kern D. Dynamic personalities of proteins. Nature 2007;450:964–972.
91. Baldwin AJ, Kay LE. NMR spectroscopy brings invisible protein states into focus. Nat Chem Biol 2009;5:808–814.
92. Bellino S, Francavilla V, Longo O, Tripiciano A, Paniccia G, Arancio A, Fiorelli V, Scoglio A, Collacchi B, Campagna M, Lazzarin A, Tambussi G, Din CT, Visintini R, Narciso P, Antinori A, D'Offizi G, Giulianelli M, Carta M, Di Carlo A, Palamara G, Giuliani M, Laguardia ME, Monini P, Magnani M, Ensoli F, Ensoli B. Parallel conduction of the phase I preventive and therapeutic trials based on the Tat vaccine candidate. Rev Recent Clin Trials 2009;4:195–204.
93. Azizi A, Diaz-Mitoma F. Viral peptide immunogens: current challenges and opportunities. J Pept Sci 2007;12:776–786.
94. Kao DJ, Hodges RS. Advantages of a synthetic peptide immunogen over a protein immunogen in the development of an anti-pilus vaccine for *Pseudomonas aeruginosa*. Chem Biol Drug Design 2009; 74:33–42.
95. Moseri A, Tantry S, Sagi Y, Arshava B, Naider F, Anglister J. An optimally constrained V3 peptide is a better immunogen than its linear homolog or HIV-1 gp120. Virology 2010;401:293–304.
96. Putkey JA, Waxham MN, Gaertner TR, Brewer KJ, Goldsmith M, Kubota Y, Kleerekoper QK. Acidic/IQ motif regulator of calmodulin. J Biol Chem 2008;283:1401–1410.
97. Barbato G, Ikura M, Kay LE, Pastor RW, Bax A. Backbone dynamics of calmodulin studied by 15N relaxation using inverse detected two-dimensional NMR spectroscopy: the central helix is flexible. Biochemistry 1992;31:5269–5278.
98. Izumi Y, Watanabe H, Watanabe N, Aoyama A, Jinbo Y, Hayashi N. Solution X-ray scattering reveals a novel structure of calmodulin complexed with a binding domain peptide from the HIV-1 matrix protein p17. Biochemistry 2008;47:7158–7166.
99. Sugita T, Yoshikawa T, Mukai Y, Yamanada N, Imai S, Nagano K, Yoshida Y, Shibata H, Yoshioka Y, Nakagawa S, Kamada H, Tsunoda SI, Tsutsumi Y. Comparative study on transduction and toxicity of protein transduction domains. Br J Pharmacol 2008;153:1143–1152.
100. Kaul M, Garden GA, Lipton SA. Pathways to neuronal injury and apoptosis in HIV-associated dementia. Nature 2001;410:988–994.
101. King JE, Eugenin EA, Buckner CM, Berman JW. HIV tat and neurotoxicity. Microbes Infect 2006;8:1347–1357.
102. Banks WA, Robinson SM, Nath A. Permeability of the blood-brain barrier to HIV-1 Tat. Exp Neurol 2005;193:218–227.
103. Nath A, Psooy K, Martin C, Knudsen B, Magnuson DS, Haughey N, Geiger JD. Identification of a human immunodeficiency virus type 1 Tat epitope that is neuroexcitatory and neurotoxic. J Virol 1996;70:1475–1480.
104. Toborek M, Lee YW, Flora G, Pu H, András IE, Wylegala E, Hennig B, Nath A. Mechanisms of the blood-brain barrier disruption in HIV-1 infection. Cell Mol Neurobiol 2005;25:181–199.
105. Karn J. Tackling tat. J Mol Biol 1999;293:235–254.

106. Pardo CA, McArthur JC, Griffin JW. HIV neuropathy: insights in the pathology of HIV peripheral nerve disease. J Peripheral Nervous Syst 2001;6:21–27.
107. Ammosova T, Washington K, Debebe Z, Brady J, Nekhai S. Dephosphorylation of CDK9 by protein phosphatase 2A and protein phosphatase-1 in Tat-activated HIV-1 transcription. Retrovirology 2005;2:1–15.
108. Zhou M, Halanski MA, Radonovich MF, Kashanchi F, Peng J, Price DH, Brady JN. Tat modifies the activity of CDK9 to phosphorylate serine 5 of the RNA polymerase II carboxyl-terminal domain during human immunodeficiency virus type 1 transcription. Mol Cell Biol 2000;20:5077–5086.
109. Chen RC, Liu M, Li H, Xue Y, Ramey WN, He NH, Ai NP, Luo HH, Zhu Y, Zhou N, Zhou Q. PP2B and PP1 alpha cooperatively disrupt 7SK snRNP to release P-TEFb for transcription in response to Ca2+ signaling. Genes Dev 2008;22:1356–1368.
110. Negulescu PA, Shastri N, Cahalan MD. Intracellular calcium dependence of gene expression in single T lymphocytes. Proc Natl Acad Sci USA 1994;91:2873–2877.
111. Poggi A, Carosio R, Rubartelli A, Zocchi MR. beta-mediated engulfment of apoptotic tumor cells by dendritic cells is dependent on CAMKII: inhibition by HIV-1 Tat. J Leukocyte Biol 2002;71:531–537.
112. Poggi A, Rubartelli A, Zocchi MR. Involvement of dihydropyridine-sensitive calcium channels in human dendritic cell function. J Biol Chem 1998;273:7205–7209.
113. Goh KC, Haque SJ, Williams BRG. p38 MAP kinase is required for STAT1 serine phosphorylation and transcriptional activation induced by interferons. EMBO J 1999;18:5601–5608.
114. Platanias LC. Mechanisms of type-I- and type-II-interferon-mediated signalling. Nat Rev Immunol 2005;5:375–386.
115. Santella L, Ercolano E, Nusco GA. The cell cycle: a new entry in the field of Ca2+ signaling. Cell Mol Life Sci 2005;62:2405–2413.
116. Li CJ, Ueda Y, Shi B, Borodyansky L, Huang LL, Li YZ, Pardee AB. Tat protein induces self-perpetuating permissivity for productive HIV-1 infection. Proc Natl Acad Sci USA 1997;94:8116–8120.
117. Wang CM, Li N, Liu XG, Zheng YY, Cao XT. A novel endogenous human CaMKII inhibitory protein suppresses tumor growth by inducing cell cycle arrest via p27 stabilization. J Biol Chem 2008;283:11565–11574.
118. Wang X, Kleerekoper QK, Xiong LW, Putkey JA. Intrinsically disordered PEP-19 confers unique dynamic properties to apo and calcium calmodulin. Biochemistry 2010;49:10287–10297.
119. McCloskey TW, Ott M, Tribble E, Khan SA, Teichberg S, Paul MO, Pahwa S, Verdin E, Chirmule N. Dual role of HIV Tat in regulation of apoptosis in T cells. J Immunol 1997;158:1014–1019.
120. Wayman GA, Lee YS, Tokumitsu H, Silva AJ, Soderling TR. Calmodulin-kinases: modulators of neuronal development and plasticity. Neuron 2008;59:914–931.